

Fietz, S., Prah, F. G., Moraleda, N., & Rosell-Melé, A. (2013). Eolian transport of glycerol dialkyl glycerol tetraethers (GDGTs) off Northwest Africa. *Organic Geochemistry*, 64, 112-118. doi:10.1016/j.orggeochem.2013.09.009

Eolian transport of glycerol dialkyl glycerol tetraethers (GDGTs) off northwest Africa

Susanne Fietz^{a,b*}, Fredrick G. Prah^c, Núria Moraleda^a, Antoni Rosell-Melé^{a,d}

^a *Institut de Ciència i Tecnologia Ambientals, Universitat Autònoma de Barcelona, 08913 Cerdanyola del Vallès, Catalonia, Spain*

^b *Stellenbosch University, Department of Earth Sciences, 7602 Stellenbosch, Western Cape, South Africa*

^c *College of Oceanic & Atmospheric Sciences, Oregon State University, Corvallis, OR 97331-5503, USA*

^d *Institució Catalana de Recerca i Estudis Avançats, 08010 Barcelona, Catalonia, Spain*

* *Corresponding author: Tel +27-21-808-3117.*

Email address: s_fietz@web.de (Susanne Fietz).

ABSTRACT

Branched glycerol dialkyl glycerol tetraethers (brGDGTs) of purportedly terrestrial origin are frequently detected in marine sediments, even in remote ocean sites where no direct impact from land erosion via rivers takes place. At these places, the most likely explanation for the presence of brGDGTs is in situ production or eolian transport, but neither possibility has been demonstrated in the open ocean. Here, we report the presence of isoprenoid (iso) and brGDGTs in eight dust samples collected off Northwest Africa. Based on previous studies, prevailing wind patterns, bulk chemistry, *n*-alkane composition and isotopic signatures, we show that Northwest Africa is the likely principal origin of the GDGTs in the dust. The concentrations of plant wax *n*-alkanes in the dust are several orders of magnitudes higher than those of GDGTs, and, based on the distributions of these two compound classes, we infer that they tag different carbon pools and sources of organic matter. Our finding demonstrates that brGDGTs and isoGDGTs in marine sediments and wind-derived deposits can have an eolian source. Consequently, climate reconstruction may be attempted from wind-derived deposits of brGDGTs, even in remote oceanic areas.

KEYWORDS: allochthonous input; eolian dust; GDGTs; *n*-alkanes; isotopic signature; mean annual air temperature (MAAT); soil organic material

RUNNING HEAD: Eolian transport of GDGTs

1. Introduction

The long-range transport of natural terrestrial organic matter (OM) takes place through the atmosphere. This long-range transport of windborne terrestrial OM has been well documented in dust and sediments from remote oceanic locations (e.g. Kawamura, 1995; Bendle et al., 2007). Several wind systems are responsible for transporting dust from the Sahara and the Sahel regions across northwestern Africa and to varying distances from the coast to the Atlantic Ocean at different times of the year (see Stuut et al., 2005). The largest amount of this dust is transported by the trade winds (NE and SW) but, during winter, most parts of North Africa are also characterized by strong near surface Harmattan trade winds (Engelstaedter et al., 2006). Dust is also transported within the African Easterly Jet (AEJ), a mid-tropospheric jet located over much of tropical northern Africa during the northern hemisphere summer. With an average periodicity of three to five days, dust is also carried by the Saharan Dust Layer (SAL) that propagates westward with the AEJ (Karyampudi and Carlson, 1988; Karyampudi et al., 1999).

The proportion by volume of the total airborne particulate matter made up by biological material in remote marine environments is estimated to be at least 10% (Matthias-Maser et al., 1997). The predominant components of the biogenic lipid fraction in oceanic aerosols are from higher plant leaf waxes (Rogge et al., 1993; Kawamura et al., 1995; Simoneit et al., 2004) airlifted by weathering and ablation, or by resuspension of ground litter (Simoneit, 1977; Conte and Weber, 2002). Other major natural constituents of the organic fraction in aerosols are saccharides and carboxylic acids that are interpreted as tracers of biomass burning and resuspended soil particles (Simoneit and Mazurek, 1982; Kawamura, 1995). There is also ample evidence for the presence of soil lipids, pollen, fungal spores, bacteria and viruses in aerosol samples (e.g. Pady and Kelly, 1953; Mathias-Maser, 1997; Shinn et al., 2000; Griffin et al., 2006). There is evidence, however, that a large proportion of the aerosol organic fraction is often not characterised and the occurrence of polar molecules may be overlooked (Alves, 2008).

We report here the occurrence of branched glycerol dialkyl glycerol tetraethers (brGDGTs) in aerosol samples. These lipids have become a focus of attention in paleoclimate research as they may provide a means of reconstructing continental surface air temperature from their analysis in marine or lacustrine sediments (Weijers et al., 2007; Rueda et al., 2009; Peterse et al., 2011). They are thought to derive from soil bacteria (Weijers et al., 2006), but have also been described in sediments from remote ocean sites, where no direct impact from land erosion via rivers takes place (Fietz et al., 2012). At these places, the most likely hypothetical explanation for the presence of brGDGTs is their in situ production by unknown organisms, or eolian transport, although neither process has been demonstrated to mediate in their generation or transport to deep open sediments. Eolian transport and redeposition of brGDGTs has been suspected for loess paleosols (Zech et al., 2012) and, considering the diversity of biological material in aerosols (Després et al., 2012), it should be expected that they contain brGDGTs. However, so far the only published analysis of GDGTs in atmospheric dust obtained by air filtration near the West coast of Central Africa reported that GDGTs were below the detection level (Hopmans et al., 2004).

2. Experimental

2.1. Sample collection

Six dust samples were collected during the RRS Shackleton cruise S4/80 Leg 1 and 6 in 1980 and 1981 (hereafter labelled “M” samples to respect cruise labelling) and two more were collected during the TAF cruise in March and July 1972 (“TAF” samples) using nylon mesh for shipboard sampling (Chester and Johnson, 1971). The samples had been stored dry at room temperature in clean glass vials. A map for the sampling locations is shown in Fig. 1 and coordinates for each ship track are given in Table 1.

2.2. Back trajectories

For each individual sample seven day back trajectories were calculated using the Hybrid Single-Particle Lagrangian Integrated Trajectory model of the National Oceanic and Atmospheric Administration (NOAA) [HYSPLIT model access available from NOAA Air Resources Laboratory Real-time Environmental Applications and Display System (READY) at <http://ready.arl.noaa.gov/HYSPLIT.php>; Draxler and Rolph, 2013]. The trajectories were generated for air masses at 10, 1500 and 5500 m above ground level using the vertical velocity model with the GDAS archive data.

2.3. Elemental and isotopic analysis of C and N

Measured bulk properties included total organic carbon (TOC) and total nitrogen (TN), as well as the stable isotopic composition of each ($\delta^{13}\text{C}_{\text{TOC}}$ and $\delta^{15}\text{N}_{\text{TN}}$). Details of bulk chemical analysis are given by Walinsky et al. (2009). Briefly, total carbon (TC) values were obtained using a Carlo Erba NA-1500 elemental analyzer. The TOC and TN content were assessed from analysis of sub-samples pre-treated to remove inorganic carbon using vapor acidification. Isotopic analysis was accomplished using the same elemental analyzer (Carlo Erba NA-1500) interfaced to a Delta XL plus isotope ratio mass spectrometer rather than a thermal conductivity detector. All stable isotopic data are reported in standard delta notation ($\delta^{13}\text{C}_{\text{‰}}$, $\delta^{15}\text{N}_{\text{‰}}$) referring to Pee Dee Belemnite (PDB) and atmospheric N_2 as the respective reference.

2.4. Lipid biomarker analysis

2.4.1. Sample extraction and clean up

Ca. 0.4 g dry dust particulate matter were extracted for each sample using microwave assisted extraction with CH_2Cl_2 :MeOH (3:1, v:v) as described by Fietz et al. (2011). A process blank sample containing extraction solvent only, and a sample containing a routine control sediment mixture were extracted in parallel with the dust samples. Extracts were fractionated into four fractions as in Bendle et al. (2006), but the samples were not saponified prior to fractionation. Glass pipettes were filled with ca. 0.5 g of 1% H_2O -deactivated silica, which before was cleaned with a 24-h Soxhlet extraction using MeOH. The columns were cleaned and conditioned with 3 ml hexane. The first fraction (F1) was eluted with 4 ml hexane, F2 with 2 ml hexane: CH_2Cl_2 (2:1, v:v), F3 with 4 ml CH_2Cl_2 and F4 with 5 ml CH_2Cl_2 :MeOH (95:5). Only F1 and F4 were analyzed. The hexane fraction (F1) contained the *n*-alkanes. F4 was used for isoprenoid (iso) and brGDGTs analysis.

2.4.2. *n*-Alkane analysis

Quantitative analysis was carried out using capillary gas chromatography with flame ionization detection as described by Prah et al. (2003). Quantification, with correction

made for analytical recovery, was accomplished using 3-methyltricosane as internal standard. Compound-specific carbon isotope analysis of *n*-alkane fractions obtained after urea adduction was accomplished using an HP6890 gas chromatograph equipped with a capillary column and interfaced to a ThermoQuest-Finnigan Delta Plus XL mass spectrometer as in Prahl et al. (2003). The *n*-alkane distribution and the $\delta^{13}\text{C}$ composition of individual components in the TAF samples have been described by Huang et al. (2000) and were not reanalyzed.

2.4.3. GDGT analysis

A Dionex P680 high performance liquid chromatography (HPLC) system coupled to a Thermo Finnigan TSQ Quantum Discovery Max triple-stage quadrupole mass spectrometer with an atmospheric pressure chemical ionization (APCI) interface (HPLC-MS) was used. The GDGTs were separated with a Tracer Excel CN column. The solvent program was modified from Schouten et al. (2007) and Escala et al. (2007). Details of the column, solvent program and APCI parameters are given by Fietz et al. (2011). GDGTs were monitored in selected ion monitoring (SIM) mode. Here, we use the mass to refer to the various GDGT molecules, i.e. brGDGT₁₀₂₂ is the branched GDGT with M^+ at m/z 1022. A sample containing the synthetic tetraether lipid “GR” (see Réthoré et al., 2007, for details) was extracted in parallel with the dust samples and used as external standard for GDGT quantification. The reproducibility of the quantification of GDGTs was estimated to be >90% (Escala, 2009).

We appraised the possibility of laboratory contamination of the samples with GDGTs, given that in a previous study they were not detected in aerosols (Hopmans et al., 2004). We did not detect GDGTs in six solvent blank runs using HPLC-MS prior to analysis of the dust extracts, so we discarded possible HPLC column carry over or system contamination as a source of the GDGTs. Furthermore, an analytical blank sample containing extraction solvent only was also extracted in parallel with the dust samples. Caldarchaeol (m/z 1302) and crenarchaeol (m/z 1292), were detected in this process blank. However, process blank caldarchaeol concentration was only 2.9% of the lowest caldarchaeol concentration measured in the dust samples; process blank crenarchaeol concentration was even lower, only 1.6% of the lowest crenarchaeol concentration measured in the dust samples. No brGDGTs were detected in the process blank. Consequently, we consider the probability of contamination artefacts in our study negligible.

3. Results and discussion

3.2 Provenance and composition of dust OM

Almost all seven day back trajectories at 1500 m (ca. 850 hPa) had tracks over NW Africa (details in Supplementary Material Part 1 and Supplementary Fig. 1). This is in line with reported observations (e.g., Schefuß et al., 2003). The back trajectories further indicate that the aerosols uplifted from northern Africa could reach the sampling sites within a few days, except for sites M1 and TAF1. We could distinguish three different types of 1500 m trajectories for the dust to the collection sites: from the Sahara (M2), the rain forest area around the west coast of Sierra Leone (M3) and the Sahel region (M4-M6 and TAF2).

Studies of dust and surface sediments off Northwest Africa have shown that the main source of eolian OM is North Africa (Simoneit et al., 1977; Huang et al., 2000; Eglinton et al., 2002; Schefuß et al., 2003). Our study is no exception in this regard, and for two of our samples (TAF1 and TAF2) Huang et al. (2000) discussed the African origin of the OM. For samples M1 to M6 we also found similar results to those in the literature for *n*-alkanes and bulk chemistry parameters at other locations. For instance the TOC content of the dust samples was relatively low, averaging 1.3% (Table 2), consistent with the content found at an offshore buoy, 2° northwards and 3° westwards from the average position of site TAF2 (Eglinton et al., 2002), and consistent with other dust samples from the same region (Huang et al., 2000). The bulk $\delta^{13}\text{C}$ values (Table 2), are again similar to those in dust deposited at the offshore buoy (Eglinton et al., 2002). These bulk $\delta^{13}\text{C}$ values were more ^{13}C depleted near the shore (Table 2; Supplementary Fig. 2) and bulk parameters for other TAF dust samples confirm the increasing carbon content and the lower isotopic composition of organic carbon towards the near shore sites, as well as increasing N contents (Supplementary Table 1; Huang et al., 2000).

Most of the *n*-alkane concentrations for the M1 to M6 samples (Table 2; Supplementary Fig. 2) and the $\delta^{13}\text{C}$ values of the odd-numbered long-chain *n*-alkanes ($\text{C}_{25}\text{-C}_{33}$; Fig. 2) are also in agreement with values for the buoy and ship track dust samples (Huang et al., 2000; Eglinton et al., 2002; Schefuß et al., 2003). The total concentration of long chain *n*-alkanes in our samples was considerably higher at the site nearest the shore than further offshore (Table 2; Supplementary Fig. 2). All dust samples exhibited a typical plant wax *n*-alkane pattern of odd long chain homologues maximizing at *n*- C_{29} or *n*- C_{31} (Fig. 2), reflected in carbon preference index (CPI) values ranging from 2.95 to 5.8 (Table 2). The dominant C chain lengths and CPI values of the *n*-alkanes confirm that the *n*-alkane signatures correspond to the collection of relatively fresh plant-derived material.

The ratio of the two dominant *n*-alkanes [$n\text{-C}_{31}/(n\text{-C}_{29}+n\text{-C}_{31})$] varies between 0.38 and 0.69 (Table 2; Supplementary Fig. 2), exhibiting a similar latitudinal trend than shown previously for the same region (16°-1°N; Schefuß et al., 2003). This *n*- C_{31} vs. *n*- C_{29} ratio, the ^{13}C -enriched TOC, and the compound specific *n*-alkane $\delta^{13}\text{C}$ values indicate a substantial source from C_4 vegetation (Eglinton et al., 2002; Schefuß et al., 2003). This relatively high contribution of C_4 plant material points towards a tropical climate source region, where temperatures would be high, water availability low and soil fertility poor (Pearcy and Ehleringer 1984; Huang et al., 2000; Schefuß et al., 2003).

In general, our data suggest a decreasing north-south, or shore-offshore amount of transported OM, and a decreasing north-south or shore-offshore trend in C_4 plant contribution (Table 2; Supplementary Fig. 2). The spatial distribution of bulk chemistry and *n*-alkane signatures probably reflects the variability in the locations of the dust sources and time of transport. In fact, the different back trajectory pathways discussed above also reflect the chemical content of the samples. For example, sample M1, i.e., the sample closest to the equator with its seven day back trajectories not crossing the continent (Supplementary Fig. 1), has $\delta^{13}\text{C}$ values for the *n*- C_{31} more than 4‰ lower than samples M2-M6, and also a much lower $n\text{-C}_{31}/(n\text{-C}_{29} + n\text{-C}_{31})$ value, but highest CPI values (Table 2; Supplementary Fig. 2). Sample M6, with back trajectory reaching the Sahel zone, has highest C_4 plant contribution and highest *n*-alkane concentrations and a high CPI value. Sample M3, in contrast, originating from the West African rain forest,

has the lowest amount of deposited OM and *n*-alkanes, the lowest CPI value, the lowest C/N value, but average C₄ plant contribution.

3.3 GDGTs in dust and their provenance

Iso- and brGDGTs were detected in all the dust samples (Table 2; Fig. 2). They were also detected in a ninth dust sample, collected in the vicinity of the Canary Islands for which we lack the exact coordinates (Supplementary Table 2, Supplementary Fig. 3). Given the likely African origin of the OM and lipids in the samples, as argued in the previous section, the same provenance most likely applies to the GDGTs. The concentration of brGDGTs (0.27 to 2.8 $\mu\text{g g C}^{-1}$; Table 2) in the dust is generally higher than that of total isoGDGTs (0.28 to 0.50 $\mu\text{g g C}^{-1}$; Table 2) and crenarchaeol (0.08 to 0.37 $\mu\text{g g C}^{-1}$), except in sample TAF2. GDGT distribution pattern (Fig. 2) found in the dust samples are similar to those found in soils of tropical and temperate regions with a dominance of brGDGTs vs. isoGDGTs and brGDGT₁₀₂₂ and brGDGT₁₀₃₆ being the most abundant GDGTs (Weijers et al., 2010; Loomis et al., 2011). The BIT index values, ranging from 0.67 to 0.91 (Table 2), are further indicative of a terrestrial source for all the dust samples (Hopmans et al., 2004).

The mean annual air temperature (MAAT) values estimated from the brGDGT indices (Peterse et al., 2012) for the dust range from 17 to 31 °C, and are highest in the sample from the southernmost open ocean site (Table 2; Supplementary Fig. 2). These brGDGT-derived MAAT values are therefore in accord with the assumption of a temperate to tropical source region for the GDGTs. The calculated TEX₈₆-derived temperature (Kim et al., 2010) based on the isoGDGT composition in the dust samples, in contrast, ranges from 34 to 42 °C (Table 2). These estimates are much higher than the sea surface temperature below the pathways followed by the dust, which varies between 20 and 27.5 °C at our collecting sites according to the World Ocean Atlas 2009 data (Locarnini et al., 2010). Therefore, we can reject the possibility that the isoGDGTs in our dust samples are derived mainly from sea spray. C-normalized brGDGT concentration correlates positively with crenarchaeol (Fig. 3), which supports a similar terrestrial source and/or transport pattern of brGDGTs and crenarchaeol and other isoGDGTs (Fietz et al., 2011).

The spatial distribution of the GDGT concentration does not show a clear latitudinal or longitudinal trend, as the lowest concentrations are found near shore and far over the open ocean, and the highest in between (Table 2; Supplementary Fig. 2). Furthermore, the compositions of iso- and brGDGTs in the samples are variable (Fig. 2). This could be interpreted as a reflection of different origin of the dust collected at the various sites. However, the compositional changes are not in full agreement with the four back trajectory groups defined above. For instance, samples M2-M4 (likely originating from the Saharan, Sahel and rain forest zones, Supplementary Fig. 1) have similar concentration and composition, which are different from those in the rest of samples (Table 2; Fig. 2). Sample M6, likely originating from a Sahel zone similar to M4 and M5, differs in amount and composition of brGDGTs and derived indices (Table 2; Fig. 2). Different air masses might, however, have other provenances. For instance, it might be worth exploring the possibility that the iso- and brGDGTs in dust originate, at least partly, from the dried up lake sediments from NW Africa and the large Chad Basin, which are known to represent a major contribution to eolian dust from NW Africa. Supplementary Fig. 1 shows a forward trajectory indicating how air masses carrying

uplifted particles from around the Chad Basin could have reached the ship track sites within the week of sampling M1 to M5.

In comparison with the concentration of *n*-alkanes, the GDGTs occur in 2-4 orders of magnitude lower concentrations in all samples. BrGDGTs concentration correlates poorly with TOC content, bulk $\delta^{13}\text{C}$ and *n*-alkane specific $\delta^{13}\text{C}$ values (Table 2; Fig. 3). BrGDGTs concentration furthermore displays an inverse nonlinear correlation with odd long chain *n*-alkanes content (Fig. 3). Backward trajectories do not necessarily lead back to the source of dust as the winds may pick up dust from local outbreaks along their pathways (Stuut et al., 2005). There is hence the possibility that a dust sample at a particular site may reflect inputs of lipids incorporated into the dust plume at different locations along the dust pathway. The negative correlation between brGDGTs and *n*-alkanes might also relate to the biogeographical differences in the source locations, which arguably expand from the Sahara and Sahel desert to the tropical rainforest zones. The *n*-alkanes derive from the epicuticular wax of vascular plants and grass, while brGDGTs derive from microbial communities in soils. Both are terrigenous materials, which, however, represent different C pools, and hence tag different components of the terrestrial biogeochemical C cycle. The dust particle composition depends on the composition at the source locations along the pathway as well as on wind strength and on the distance to the site of deposition (Stuut et al., 2005). Spatial and seasonal variability in the climatic conditions at the source locations as well as in seasonal wind trajectories and their strength might further contribute to the diffuse distribution and cause the weak relationship between GDGT concentration and bulk chemistry.

4. Conclusions

Iso- and brGDGTs have been detected in dust samples off Northwest Africa. It is well accepted that the atmosphere is a major pathway for the transport of allochthonous OM and microscopic organisms to the ocean, originating partly from resuspended soil. It is therefore not entirely surprising that dust contains, as shown here, lipids such as GDGTs, which are abundant in terrestrial settings. The GDGTs in the dust samples most likely originate from subtropical and tropical Africa, as inferred from previous studies of lipids in aerosols and sediments from the northeast Atlantic, and complementary data on *n*-alkanes and GDGT indices obtained here. The lack of correlation between GDGT concentration, their indices and *n*-alkanes is interpreted as evidence that the two classes of lipids tag a different pool of OM whose major source locations might be different as well. Our finding thus demonstrates that GDGTs in remote ocean sediments, i.e. settings with no significant continental fluvial input, will probably have a contribution from eolian terrestrial origin. Therefore, brGDGTs might serve as important additional dust tracers in future paleoenvironmental studies.

Acknowledgements

The authors thank K-U. Hinrichs, J.R. Maxwell and an anonymous reviewer for constructive comments. The authors gratefully acknowledge the NOAA Air Resources Laboratory (ARL) for provision of the HYSPLIT transport and dispersion model and/or READY website (<http://ready.arl.noaa.gov>). S.F. thanks the Spanish Ministerio de Ciencia e Innovación for a Juan de la Cierva fellowship. A.R.M. acknowledges funding support from the European Commission (Marie Curie-IOF, 235626; and Past4Future projects 243908) and Spanish Ministerio de Economía y Competitividad (CTM2009-12214). F.P. thanks the U.S. National Science Foundation (OCE-961685) for prior support that ultimately benefited the work.

References

- Alves, C.A., 2008. Characterisation of solvent extractable organic constituents in atmospheric particulate matter: an overview. *Anais Da Academia Brasileira De Ciencias* 80, 21-82.
- Bendle, J., Kawamura, K., Yamazaki, K., 2006. Seasonal changes in stable carbon isotopic composition of n-alkanes in the marine aerosols from the western North Pacific: Implications for the source and atmospheric transport. *Geochimica et Cosmochimica Acta* 70, 13-26.
- Bendle, J., Kawamura, K., Yamazaki, K., Niwai, T., 2007. Latitudinal distribution of terrestrial lipid biomarkers and n-alkane compound-specific stable carbon isotope ratios in the atmosphere over the western Pacific and Southern Ocean. *Geochimica et Cosmochimica Acta* 71, 5934-5955.
- Chester, R., Johnson, L.R., 1971. Atmospheric dusts collected off the west African coast. *Nature* 229, 1105-107.
- Conte, M.H., Weber J.C., 2002. Long-range atmospheric transport of terrestrial biomarkers to the western North Atlantic, *Global Biogeochemical Cycles* 16, 1142.
- Després, V., Huffman, J., Burrows, S., Hoose, C., Safatov, A., Buryak, G., Fröhlich-Nowoisky, J., Elbert, W., Andreae, M., Pöschl, U., Jaenicke R., 2012. Primary biological aerosol particles in the atmosphere: a review. *Tellus B* 64.
- Draxler, R.R., Rolph, G.D., 2013. HYSPLIT (HYbrid Single-Particle Lagrangian Integrated Trajectory) Model access via NOAA ARL READY Website (<http://ready.arl.noaa.gov/HYSPLIT.php>). NOAA Air Resources Laboratory, Silver Spring, MD.
- Eglinton, T.I., Eglinton, G., Dupont, L., Shalkovitz, E.R., Montluçon, D., Reddy, C.M., 2002. Composition, age, and provenance of organic matter in NW African dust over the Atlantic Ocean. *Geochemistry, Geophysics, Geosystems* 3, 1-27.
- Engelstaedter, S., Tegen, I., Washington, R., 2006. North African dust emissions and transport. *Earth-Science Reviews* 79, 73-100.
- Escala, M., Rosell-Melé A., Masqué P., 2007. Rapid screening of glycerol dialkyl glycerol tetraethers in continental Eurasia samples using HPLC/APCI-ion trap mass spectrometry. *Organic Geochemistry* 38, 161-164.
- Escala, M., 2009. Application of tetraether membrane lipids as proxies for continental climate reconstruction in Iberian and Siberian lakes. Ph. D. thesis, Universitat Autònoma de Barcelona (<http://www.tdx.cat/TDX-1020109-144857>).
- Fietz, S., Martínez-García, A., Hugué, C., Rueda, G., Rosell-Melé A., 2011. Constraints in the application of the Branched and Isoprenoid Tetraether index as a terrestrial input Proxy. *Journal of Geophysical Research* 116, C10032.
- Fietz, S., Hugué, C., Bendle, J., Escala, M., Gallacher, C., Herfort, L., Jamieson, R., Martínez-García, A., McClymont, E., Peck, V., Prahl, F., Rossi, S., Rueda, G., Sanson-Barrera, A. & Rosell-Melé, A., 2012. Co-variation of crenarchaeol and branched GDGTs in globally-distributed marine and freshwater sedimentary archives. *Global Planetary Change* 92/93, 275-285.
- Griffin, D.W., Westphal, D.L., Gray, M.A., 2006. Airborne microorganisms in the African desert dust corridor over the mid-Atlantic ridge, Ocean Drilling Program, Leg 209. *Aerobiologia* 22, 211-226.
- Hopmans, E.C., Weijers, J.W.H., Schefuß, E., Herfort, L., Sinninghe Damsté, J.S., Schouten S., 2004. A novel proxy for terrestrial organic matter in sediments based on branched and isoprenoid tetraether lipids. *Earth Planetary Science Letters* 224, 107-116.
- Huang, Y., Dupont, L., Sarnthein, M., Hayes, J.M., Eglinton, G., 2000. Mapping of C₄ plant input from northwest Africa into northeast Atlantic sediments, *Geochimica et Cosmochimica Acta* 64, 3505- 3513.
- Karyampudi, V.M., Carlson, T.N., 1988. Analysis and numerical simulations of the Saharan air layer and its effect on easterly wave disturbances. *Journal of the Atmospheric Sciences* 45, 3102-3136.
- Karyampudi, V.M., Palm, S.P., Reagen, J.A., Fang, H., Grant, W.B., Hoff, R.M., Moulin, C., Pierce, H.F., Torres, O., Browell, E.V., Melfi, S.H., 1999. Validation of the Saharan dust plume conceptual model using lidar, Meteosat, and ECMWF data. *Bulletin of the American Meteorological Society* 80, 1045-1075.
- Kawamura, K., 1995. Land-derived lipid class compounds in the deep-sea sediments and marine aerosols from North Pacific, In: Sakai, H., Nozaki, Y. (Eds.), *Biogeochemical Processes and Ocean Flux in the Western Pacific*. Terra Scientific Publishing Company, pp. 31-51.
- Kim, J.-H., Meer, J.v.d., Schouten, S., Helmke, P., Willmott, V., Sangiorgi, F., Koç, N., Hopmans, E.C., Sinninghe Damsté, J.S., 2010. New indices and calibrations derived from the distribution of crenarchaeol isoprenoid tetraether lipids: implications for past sea surface temperature reconstructions. *Geochimica et Cosmochimica Acta* 74, 4639-4654.

- Locarnini, R. A., Mishonov A. V., Antonov J. I., Boyer T. P., and Garcia H. E., 2010. World Ocean Atlas 2009, Volume 1: Temperature, In: S. Levitus (Ed.), NOAA Atlas NESDIS 68. U.S. Government Printing Office, Washington, D.C., 184 pp.
- Loomis, S. E., Russell, J. M., and Sinninghe Damsté, J. S.: Distributions of branched GDGTs in soils and lake sediments from western Uganda: Implications for a lacustrine paleothermometer, *Organic Geochemistry* 42, 739–751, 2011.
- Matthias-Maser, S., Krämer, M., Brinkmann, J., Schneider, W., 1997. A contribution of primary biological aerosol particles as insoluble component to the atmospheric aerosol over the south Atlantic ocean. *Journal of Aerosol Science* 28, Supplement 1, 3-4.
- Pady, S.M., Kelly, C.D., 1953. Numbers of fungi and bacteria in transatlantic air. *Science* 117, 607-609.
- Pearcy, R.W., Ehleringer, J., 1984. Comparative ecophysiology of C₃ and C₄ plants. *Plant Cell Environment* 7, 1–13.
- Peterse, F., Prins, M.A., Beets, C.J., Troelstra, S.R., Zheng, H., Gu, Z., Schouten, S., Damsté, J.S.S., 2011. Decoupled warming and monsoon precipitation in East Asia over the last deglaciation. *Earth and Planetary Science Letters* 301, 256-264.
- Peterse, F., van der Meer, J., Schouten, S., Weijers, J.W.H., Fierer, N., Jackson, R.B., Kim, J.-H., Sinninghe Damsté, J.S., 2012. Revised calibration of the MBT–CBT paleotemperature proxy based on branched tetraether membrane lipids in surface soils. *Geochimica et Cosmochimica Acta* 96, 215–229.
- Prahl, F.G., Cowie, G.L., De Lange G.J., Sparrow M.A., 2003. Selective organic matter preservation in ‘‘burn-down’’ turbidites on the Madeira Abyssal Plain, *Paleoceanography* 18, 1052.
- Réthoré, G., Montier, T., Le Gall, T., Delépine, P., Cammas-Marion, S., Lemiègre, L., Lehn, P., Benvegnu, T., 2007. Archaeosomes based on synthetic tetraether-like lipids as novel versatile gene delivery systems. *Chemical Communications* 28, 2054–2056.
- Rogge, W.F., Hildemann, L.M., Mazurek, M.A., Cass, G.R., Simoneit, B.R.T., 1993. Sources of fine organic aerosol. 4. Particulate abrasion products from leaf surfaces of urban plants. *Environmental Science and Technology* 27, 2700-2711.
- Rueda, G., Rosell-Melé, A., Escala, M., Gyllencreutz, R., Backman, J., 2009. Comparison of instrumental and GDGT-based estimates of sea surface and air temperatures from the Skagerrak. *Organic Geochemistry* 40, 287-291.
- Schefuß, E., Ratmeyer, V., Stuut, J.-B. W., Jansen, J.H.F., Sinninghe Damsté, J.S., 2003. Carbon isotope analysis of n-alkanes in dust from the lower atmosphere over the central eastern Atlantic. *Geochimica et Cosmochimica Acta* 67, 1757-1767.
- Schlitzer, R., Ocean Data View, <http://odv.awi.de>, 2013.
- Shinn, E.A., Smith, G.W., Prospero, J.M., Betzer, P., Hayes, M.L., Garrison, V., Barber, R.T., 2000. African dust and the demise of Caribbean Coral Reefs. *Geophysical Research Letters* 27, 3029-3032.
- Schouten, S., Hopmans, E.C., Schefuß, E., Sinninghe Damsté, J.S., 2002. Distributional variations in marine crenarchaeotal membrane lipids: a new organic proxy for reconstructing ancient sea water temperatures? *Earth and Planetary Science Letters* 204, 265–274.
- Schouten, S., Hugué C., Hopmans E.C., Kienhuis M., Sinninghe Damsté J.S., 2007. Analytical methodology for TEX₈₆ paleothermometry by high-performance liquid chromatography/atmospheric pressure chemical ionization-mass spectrometry, *Analytical Chemistry* 79, 2940–2944.
- Simoneit, B.R.T., 1977. Organic matter in eolian dusts over the Atlantic Ocean. *Marine Chemistry* 5, 443-464.
- Simoneit, B.R.T., Mazurek, M.A., 1982. Organic matter of the troposphere. II. Natural background of biogenic lipid matter in aerosols over the rural western United States. *Atmospheric Environment* 16, 2139-2159.
- Simoneit, B.R.T., Chester, R., Eglinton, G. 1977. Biogenic lipids in particulates from the lower atmosphere over the eastern Atlantic. *Nature* 267, 682-685.
- Simoneit, B.R.T., Kobayashi, M., Mochida, M., Kawamura, K., Lee, M., Lim, H.-J., Turpin, B.J., Komazaki, Y., 2004. Composition and major sources of organic compounds of aerosol particulate matter sampled during the ACE-Asia campaign. *Journal of Geophysical Research: Atmospheres* 109, D19S10.
- Stuut, J.-B., Zabel, M., Ratmeyer, V., Helmke, P., Schefuß, E., Lavik, G., Schneider, R., 2005. Provenance of present-day eolian dust collected off NW Africa, *Journal of Geophysical Research: Atmospheres* 110, D04202.
- Walinsky S.E., Prahl F.G., Mix A.C., Finney B.P., 2009. Distribution and composition of organic matter in coastal southeast Alaskan surface sediments. *Continental Shelf Research* 29, 1565-1579.

- Weijers, J.W.H., Schouten, S., Spaargaren, O., Sinninghe Damsté, J.S., 2006. Occurrence and distribution of tetraether membrane lipids in soils: Implications for the use of the TEX₈₆ proxy and the BIT index. *Organic Geochemistry* 37, 1680-1693.
- Weijers, J.W.H., Schouten, S., van den Donker, J.C., Hopmans, E.C., Sinninghe Damsté, J.S., 2007. Environmental controls on bacterial tetraether membrane lipid distribution in soils. *Geochimica et Cosmochimica Acta* 71, 703-713.
- Weijers, J.W.H., Wiesenberg, G.L.B., Bol, R., Hopmans, E.C., Pancost, R.D., 2010. Carbon isotopic composition of branched tetraether membrane lipids in soils suggest a rapid turnover and a heterotrophic life style of their source organism(s). *Biogeosciences* 7, 2959–2973.
- White, F., 1983. The vegetation of Africa - A descriptive memoir to accompany the UNESCO/AETFAT/UNSO Vegetation Map of Africa, Natural Resources Research Report 20, UNESCO, Paris.
- Zech, R., Gao, L., Tarozo, R., Huang Y., 2012. Branched glycerol dialkyl glycerol tetraethers in Pleistocene loess-paleosol sequences: Three case studies. *Organic Geochemistry* 53, 38–44.
- Zhao, M.X., Dupont, L., Eglinton, G., Teece, M., 2003. *n*-Alkane and pollen reconstruction of terrestrial climate and vegetation for N.W. Africa over the last 160 kyr. *Organic Geochemistry* 34, 131-143.

TABLES

Table 1

Locations and times of dust sampling: Start, end and mid-transect (average, Avg.) coordinates, plus date of collection (end point).

Location	Collection Date	Start Lat. (°N)	Start Long. (°W)	End Lat. (°N)	End Long. (°W)	Avg. Lat. (°N)	Avg. Long. (°W)
M1	31/03/1981	0.17	30.45	3.33	29.48	1.75	29.97
M2	01/04/1981	3.45	29.43	4.72	28.92	4.08	29.18
M3	01/04/1981	4.72	28.92	6.93	28.12	5.83	28.52
M4	02/04/1981	6.93	28.12	10.77	26.70	8.85	27.41
M5	03/04/1981	11.90	25.28	14.23	23.97	13.07	24.63
M6	15/11/1980	16.78	21.13	11.15	23.38	13.97	22.26
TAF1	04/04/1972	15.77	17.83	9.78	16.32	12.78	17.08
TAF2	14/07/1972	13.33	17.22	17.78	17.70	15.56	17.46

Table 2

(A) Bulk chemistry and *n*-alkanes data and (B) iso- and brGDGT concentration and indices, and GDGT-based temperature estimates.

(A) ^a	TOC (%) ^b	TN (%) ^c	C/N	$\delta^{13}\text{C}_{\text{TOC}}$ (‰)	$\delta^{15}\text{N}_{\text{TN}}$ (‰)	<i>n</i> -Alkanes ($\mu\text{g gC}^{-1}$)	<i>n</i> -Alkane CPI ^d	$\text{C}_{31}/(\text{C}_{29}+\text{C}_{31})$	$\delta^{13}\text{C}_{31}$ (‰)
M1	1.30	0.118	12.8	-18.2	5.7	1610	5.83	0.38	-31.3
M2	1.14	0.125	10.7	-17.2	8.2	705	4.54	0.55	-27.3
M3	0.54	0.125	5.1	-16.2	5.7	275	2.95	0.55	-27.1
M4	1.04	0.125	9.7	-16.2	6.1	515	4.17	0.54	-27.2
M5	1.44	0.118	14.2	-20.2	5.3	1610	4.38	0.54	
M6	1.57	0.123	14.9	-19.5	7.2	5030	5.46	0.69	-26.0
TAF1	1.59	0.143	13.0	-21.7	6.0	-	-	-	-
TAF2	1.66	0.143	13.5	-19.1	3.8	-	-	-	-
Avg.	1.3	0.13	11.7	-18.5	6.0	1630	4.6	0.5	-27.8

(B)	isoGDGTs ($\mu\text{g gC}^{-1}$)	brGDGTs ($\mu\text{g gC}^{-1}$)	TEX ₈₆ ^e	BIT ^f	MBT ^g	CBT ^g	TEX ₈₆ -T (°C) ^h	MAAT (°C) ^g	pH ^g
M1	0.30	0.52	0.80	0.78	1.04	0.38	38.2	30.7	7.1
M2	0.46	1.94	0.79	0.88	0.69	0.65	38.1	18.3	6.5
M3	0.50	2.83	0.84	0.91	0.66	0.68	41.7	17.4	6.6
M4	0.49	2.48	0.82	0.89	0.66	0.68	39.8	17.4	6.5
M5	0.42	0.87	0.79	0.79	0.78	0.49	37.4	22.4	7.0
M6	0.25	0.74	0.82	0.87	0.86	0.60	40.2	24.3	6.8
TAF1	0.40	1.20	0.77	0.91	0.66	-	36.4	21.4	-
TAF2	0.50	0.27	0.75	0.67	0.64	-	34.3	20.7	-
Avg.	0.41	1.4	0.80	0.84	0.75	0.58	38.3	21.6	6.8

^a Additional information on bulk chemistry and compound specific isotopic signatures are available for three more samples from the TAF series, shown in Supplementary Table 1; a single sample was collected from the vicinity of the Canary Islands off the West African coast, with no exact coordinates available; these results are shown in Supplementary Table 2; ^b total organic carbon; ^c total nitrogen; ^d $\text{CPI}_{(n\text{-alkanes})} = 1/2 \times [(\Sigma\text{C}_{25-33} \text{ odd}) + (\Sigma\text{C}_{27-35} \text{ odd})] / (\Sigma\text{C}_{27-35} \text{ even})$; ^e according to Schouten et al. (2002); ^f according to Hopmans et al. (2004); ^g according to Peterse et al. (2012); ^h according to core top calibration in Kim et al. (2010); TEX₈₆^H-derived temperatures averaged 32°C (range: 29.9 to 33.5 °C).

FIGURES

Fig. 1. Sampling locations: (A) global view and (B) zoom in on sampling area. Circles indicate start and end points of dust collection. Labels refer to those locations in Table 1. Solid arrows indicate direction of respective transects. Also indicated are major modern vegetation zones (White 1983) and major wind belts. Dashed dark arrows indicate year-round NE and SE trades. Dashed fine lined gray arrows indicate Harmattan wind that carries dust in winter from Northern Nigeria and Lake Chad areas when the Intertropical Convergence Zone (ITCZ) is in the southernmost position and the periodically occurring Saharan Dust Layer. Open arrows indicate zonal winds at ca. 3000 m altitude (African Easterly Jet). Graphics created using (A) Google Earth (© 2011 Google) and (B) Ocean Data View (Schlitzer, 2001). Wind systems are drawn after Huang et al. (2000), Eglinton et al. (2002), Schefuß et al. (2003) and Zhao et al. (2003) and references therein. A colour version of the map is available in the online version of this article.

Fig. 2. GDGT (A) and *n*-alkane (B) composition for dust samples (% of total concentration, where all y-axes are scaled from 0 to 50%). Codes refer to locations detailed in Table 1 and Fig. 1. Dashed line in (A) indicates separation from iso- (left) and br- (right) GDGTs. The brGDGTs 1048 and 1046 were omitted because they were not detected. (C) *n*-Alkane specific $\delta^{13}\text{C}$ values for the most prominent odd-numbered homologues. A single sample was collected additionally from the vicinity of the the Canary Islands off the Northwest African coast, with no exact coordinates available; these results are shown in Supplementary Fig. 3.

Fig. 3. Correlation plots of brGDGTs vs. (A) TOC (B) $\delta^{13}\text{C}$ -TOC, (C) odd-numbered long chain *n*-alkanes and (D) crenarchaeol.

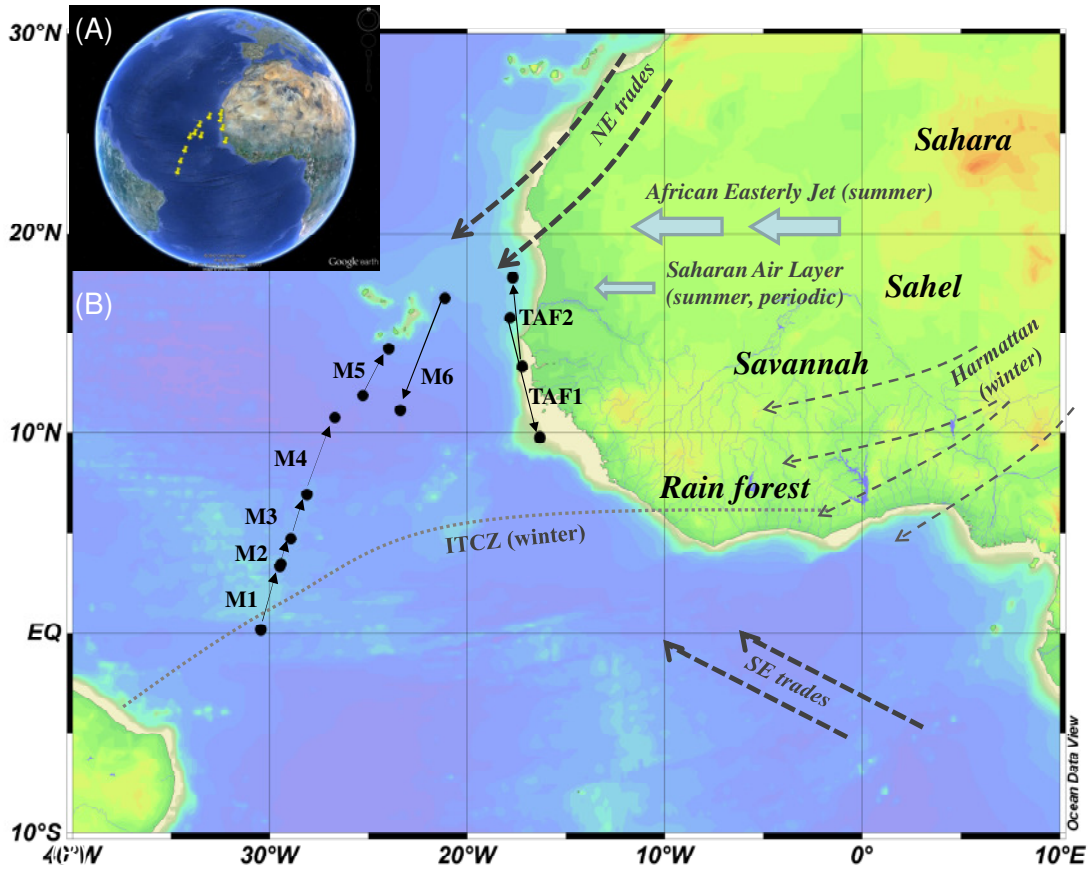


Figure 1.

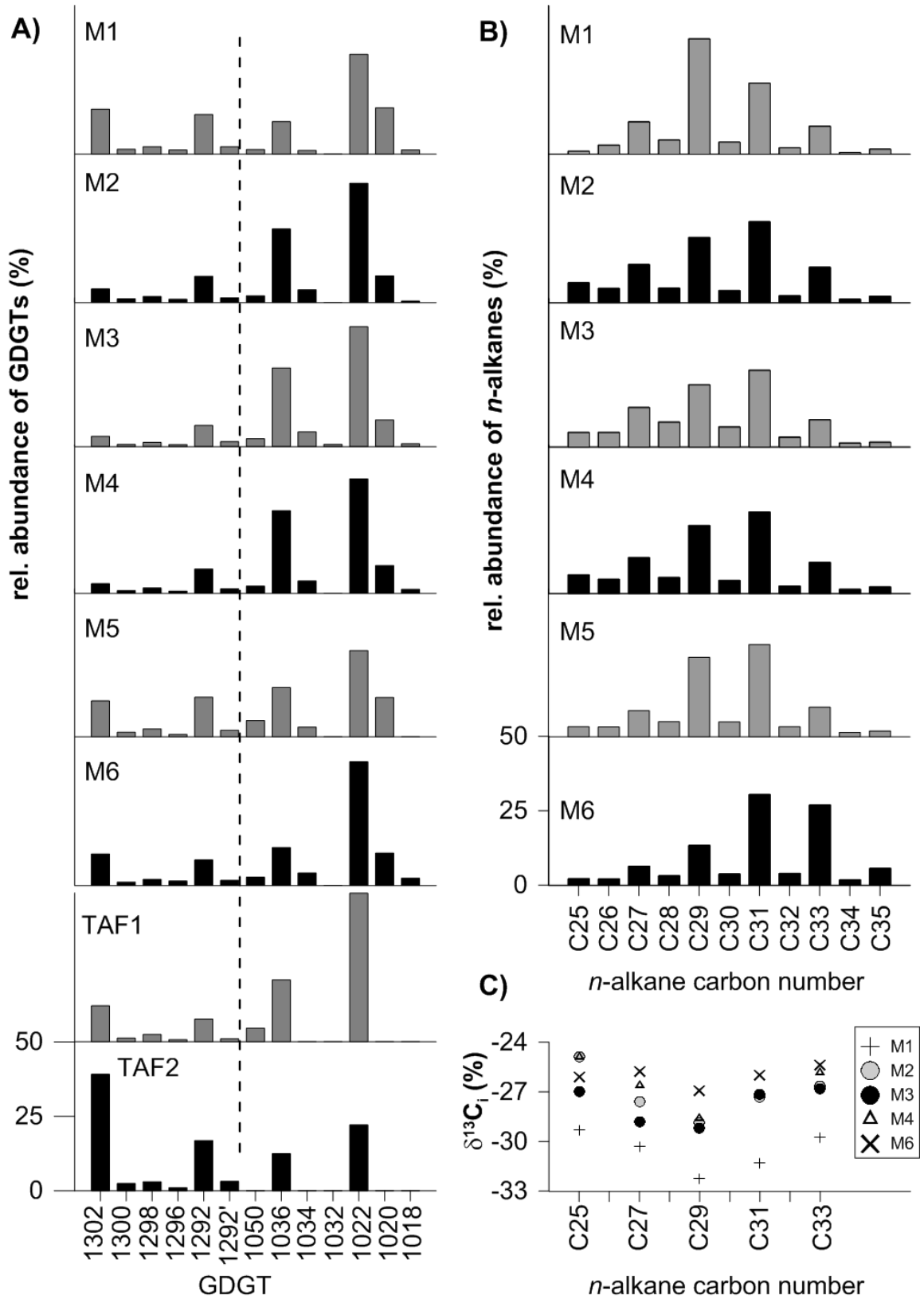


Figure 2

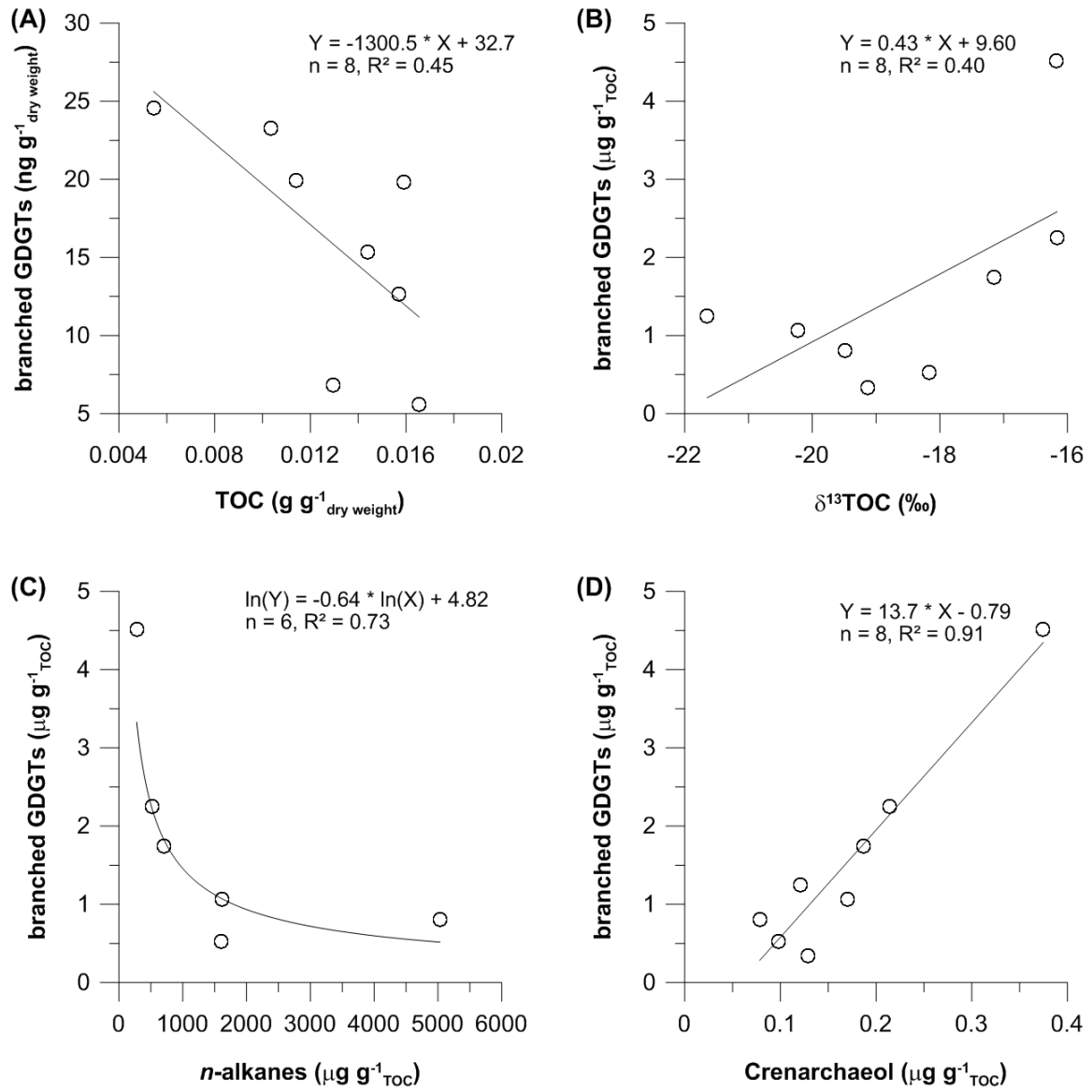


Figure 3.

Organic Geochemistry

Supplementary information for

Eolian transport of glycerol dialkyl glycerol tetraethers (GDGTs) off northwest Africa

Susanne Fietz^{a,b*}, Fredrick G. Prahl^c, Núria Moraleda^a, Antoni Rosell-Melé^{a,d}

^a *Institut de Ciència i Tecnologia Ambientals, Universitat Autònoma de Barcelona, 08913 Cerdanyola del Vallès, Catalonia, Spain*

^b *Stellenbosch University, Department of Earth Sciences, 7602 Stellenbosch, Western Cape, South Africa*

^c *College of Oceanic & Atmospheric Sciences, Oregon State University, Corvallis, OR 97331-5503, USA*

^d *Institució Catalana de Recerca i Estudis Avançats, 08010 Barcelona, Catalonia, Spain*

* *Corresponding author: Tel +27-21-808-3117.*

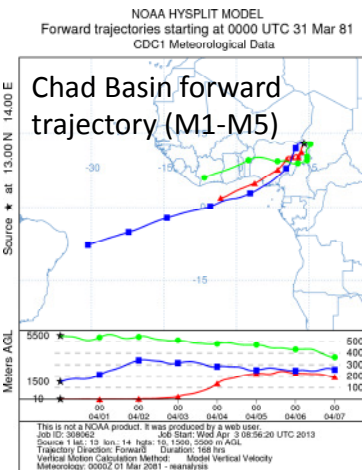
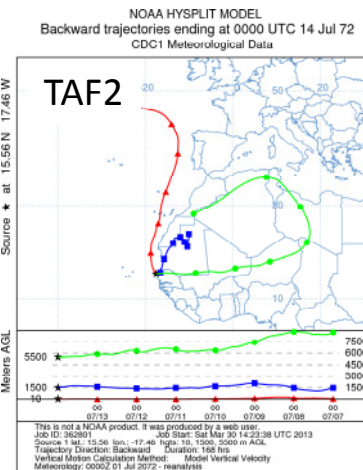
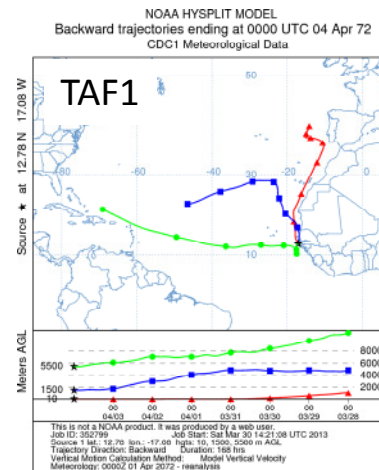
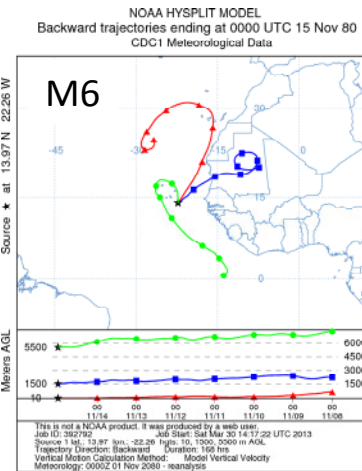
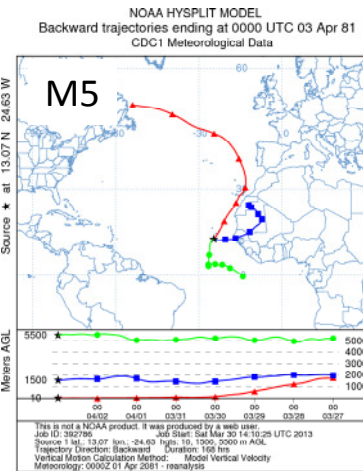
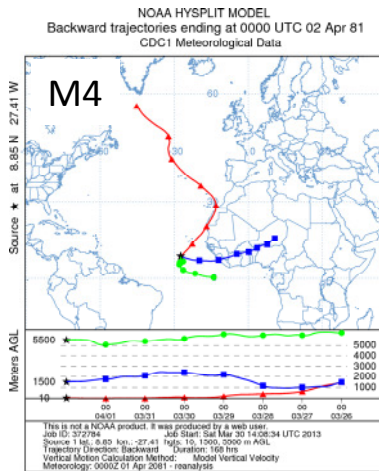
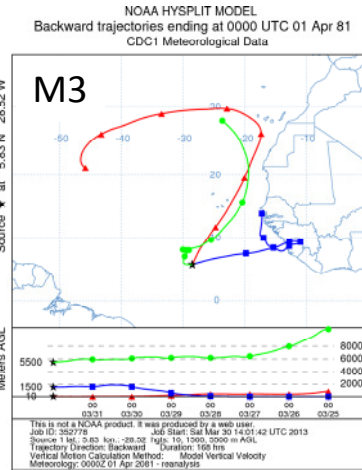
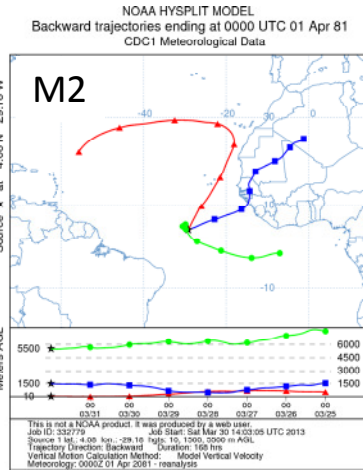
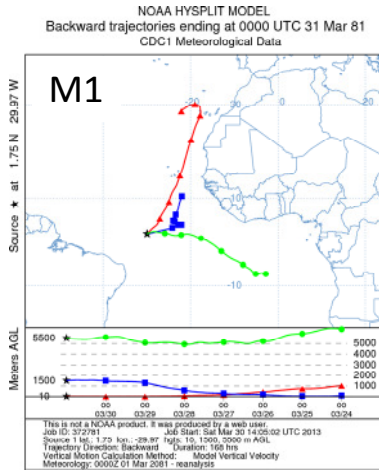
Email address: s_fietz@web.de (Susanne Fietz).

Part I. Dust provenance based on individual back trajectories of air masses

Several wind systems are recognized for dust transport across NW Africa and into the Atlantic Ocean (Stuut et al., 2005), but considerable interannual, intraseasonal and interseasonal variability drive strength and speed, especially of the African Easterly Jet, the Sahara Dust Layer and the Harmattan wind. Thus, particle load and transport depend on time and location. Back trajectories indicate the most likely sources of the particles in the respective dust samples (Supplementary Fig. 1).

Almost all back trajectories at 1500 m (ca. 850 hPa) had tracks over NW Africa (Supplementary Fig. 1). This is in line with reported observations (e.g., Schefuß et al., 2003). The back trajectories further indicate that the aerosols uplifted from northern Africa could reach the sampling sites within a few days. It is likely, however, that the sources of dust were different for the different samples. We could distinguish four different types of 1500 m trajectories for the dust to the sites: The 1500 m seven day back trajectories for M2 originated from the Sahara, for M3 from the rain forest area around the west coast of Sierra Leone, and for M4-M6 and TAF2 from the Sahel zones in Niger (M4) and Mauritania (M5, M6, and TAF2). At sites M1, M2 and M3 the 1500 m air mass path went relatively near the ground, whereas the onset for M4-M6 and both TAF samples was at >1000 m in height (Supplementary Fig. 1, lower panels). The OM characteristics likely reflect this variation in the source location and air mass paths.

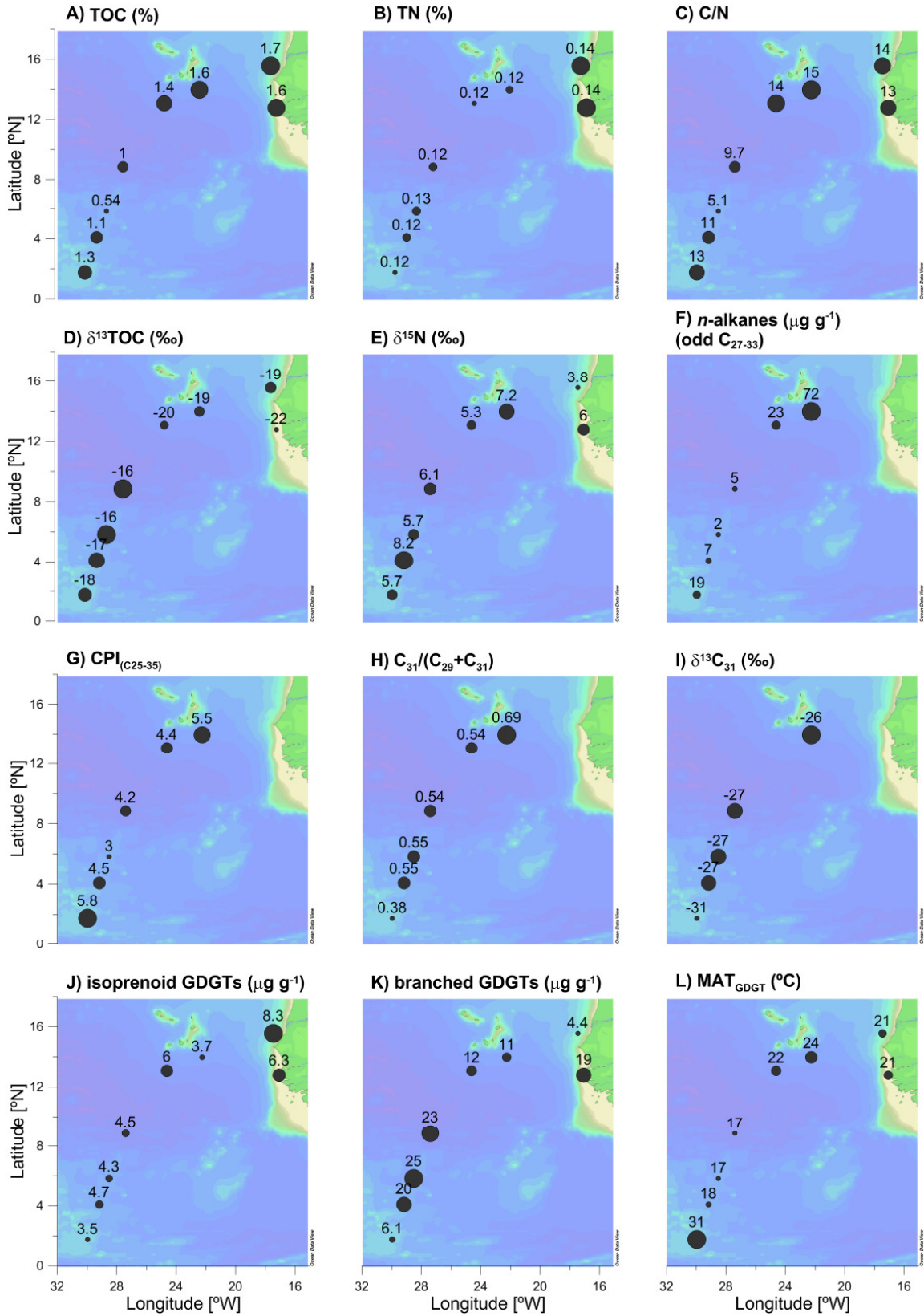
Supplementary Fig. 1. Back trajectories. For each individual sample seven day back trajectories were calculated using the Hybrid Single-Particle Lagrangian Integrated Trajectory model of the National Oceanic and Atmospheric Administration (NOAA) [HYSPLIT model access available from NOAA Air Resources Laboratory Real-time Environmental Applications and Display System (READY) at <http://ready.arl.noaa.gov/HYSPLIT.php>; Draxler and Rolph, 2013]. The trajectories were generated for air masses at 10, 1500 and 5500 m above ground level using the vertical velocity model with the GDAS archive data, 10 m being chosen as the approximate height of onboard dust collection. A height of 1.5 km corresponds roughly to the 850 hPa level, which is usually above the atmospheric boundary layer, and 5.5 km roughly to the level of 500 hPa. The heights of the back trajectories for our collecting sites fall within the air masses most likely to carry dust over the North Atlantic as mineral dust plumes blown from NW Africa are found mostly above the trade wind inversion (at 500 hPa) or in the trade wind layer (at 850 hPa; Carlson and Prospero, 1972; Schefuß et al., 2003). One forward trajectory has been calculated indicating how air masses carrying uplifted particles from around the Chad Basin could have reached the ship track sites within the week of sampling M1 to M5.



Part II. Spatial distribution of bulk organic matter, *n*-alkanes, and GDGTs

Supplementary Fig. 2. (A-E) Bulk chemistry; (F-I) *n*-alkanes data; (J-L) iso- and brGDGT concentration and related indices, and GDGT-based temperature estimates; (H) ratio of the *n*-C₃₁ to the sum of the *n*-C₂₉ and *n*-C₃₁ alkane according to Schefuß et al. (2003); (L) GDGT-based calculated mean annual temperature (MAAT) according to Peterse et al. (2012). Bubbles are placed at average latitudes over the respective sampling transect (see main article Fig. 1 for transects and Table 1 for exact start and end locations). Circle radius ranges are defined by the respective data ranges with largest circles indicating maxima and smallest circles indicating minima. Labels indicate respective site values, details given in main article Tables 2 and 3.

Additional information on bulk chemistry and compound specific isotopic signatures is available for three more samples from the TAF series, shown in Supplementary Table 1. A single sample was furthermore collected from the vicinity of the the Canary Islands off the Northwest African coast, but no exact coordinates are available. Results are shown in Supplementary Table 2.



Part III. Additional bulk chemistry data from TAF sample series

For some dust samples not enough material was left to perform GDGT and *n*-alkane analyses. However, TOC, TN and isotopic signature information is available and shown here as supplementary information in Supplementary Table 1.

Supplementary Table 1. TOC, TN and isotopic signature for the dust samples included in the main text and three additional dust samples from the TAF series (marked in red). Mid-transect (average, Avg.) coordinates and date of collection (end point) are included where available.

Locations	Collection Date	Avg. Lat. (°N)	Avg. Long. (°W)	TOC (%) ^a	TN (%) ^b	C/N	$\delta^{13}\text{C}_{\text{TOC}}$ (‰)	$\delta^{15}\text{N}_{\text{TN}}$ (‰)
Collier	1972/07/14	-	-	0.93	0.137	8.0	-16.6	8.7
M1	1981/03/31	1.75	29.97	1.30	0.118	12.8	-18.2	5.7
M2	1981/04/01	4.08	29.18	1.14	0.125	10.7	-17.2	8.2
M3	1981/04/01	5.83	28.52	0.54	0.125	5.1	-16.2	5.7
M4	1981/04/02	8.85	27.41	1.04	0.125	9.7	-16.2	6.1
M5	1981/04/03	13.07	24.63	1.44	0.118	14.2	-20.2	5.3
M6	1980/11/15	13.97	22.26	1.57	0.123	14.9	-19.5	7.2
TAF1	1972/04/04	12.78	17.08	1.59	0.143	13.0	-21.7	6.0
TAF2	1972/07/14	15.56	17.46	1.66	0.143	13.5	-19.1	3.8
TAF3	1972/07/14	12.58	17.33	1.59	0.175	10.6	-19.7	2
TAF4	1972/07/15	22.21	17.15	4.69	0.357	15.3	-23.5	3.2
TAF5	1972/07/16	26.53	15.97	9.03	0.677	15.6	-25.4	4.3
average				2.2	0.2	11.9	-19.4	5.5

^a total organic carbon; ^b total nitrogen.

Part IV. Collier dust sample

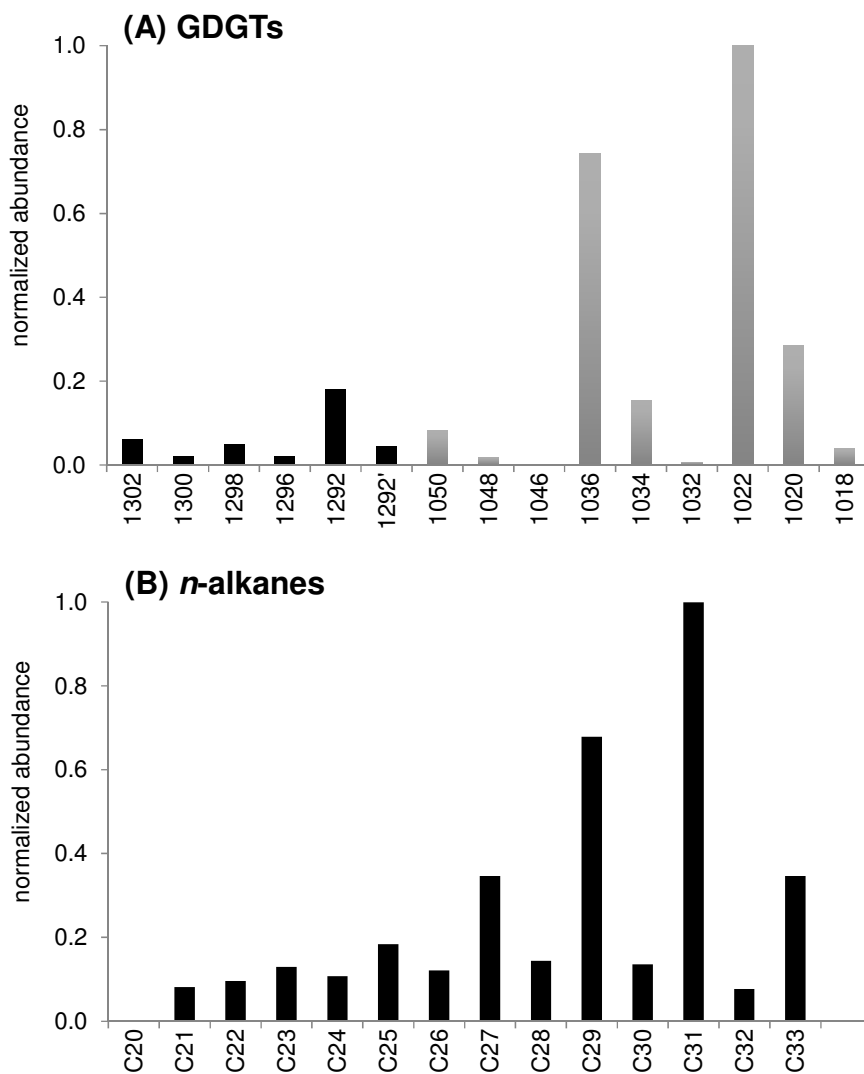
Within the dust sample set shown in the main text, a sample collected from the vicinity of the the Canary Islands off the Northwest African coast (Prah1 et al., 1997, 2003) was analyzed. Here (Supplementary Table 2 and Supplementary Figure 3) we show data for this single sample for comparison.

Supplementary Table 2. (A) Bulk chemistry and *n*-alkanes data and (B) iso and brGDGT concentration and indices, and GDGT-based temperature estimates.

(A)	TOC (%) ^a	TN (%) ^b	C/N	$\delta^{13}\text{C}_{\text{TOC}}$ (‰)	$\delta^{15}\text{N}$ (‰)	<i>n</i> -Alkanes ($\mu\text{g gC}^{-1}$)	<i>n</i> -Alkane CPI ^c	$\text{C}_{31}/(\text{C}_{29}+\text{C}_{31})$	$\delta^{13}\text{C}_{31}$ (‰)
	0.93	0.14	7.97	-16.59	8.70	250	2.65	0.57	-26.3
(B)	isoGDGTs ($\mu\text{g gC}^{-1}$)	brGDGTs ($\mu\text{g gC}^{-1}$)	TEX ₈₆ ^d	BIT ^e	MBT ^f	CBT ^f	TEX ₈₆ -T (°C) ^g	MAAT (°C) ^f	pH ^f
	0.77	5.33	0.84	0.92	0.69	0.60	42.1	18.6	6.65

^a total organic carbon; ^b total nitrogen; ^c $\text{CPI}_{(n\text{-alkanes})} = 1/2 \times [(\sum\text{C}_{25-33} \text{ odd}) + (\sum\text{C}_{27-35} \text{ odd})] / (\sum\text{C}_{27-35} \text{ even})$; ^d according to Schouten et al. (2002); ^e according to Hopmans et al. (2004); ^f according to Peterse et al. (2012); ^g according to core top calibration in Kim et al. (2010); TEX₈₆^H-derived temperature was 33.5 °C.

Supplementary Fig. 3. Distribution diagrams of (A) GDGTs and (B) long chain *n*-alkanes (from Prahl et al., 1997). The numbers on the x-axis in (A) represent the *m/z* of the respective GDGT, with 1292' indicating the crenarchaeol regioisomer. The numbers on the x-axis in (B) indicate the C chain length. In (A) black bars indicate iso- and gray bars brGDGTs.



References

- Carlson T.N., Prospero J.M., 1972. The large-scale movement of Saharan air outbreaks over the equatorial North Atlantic. *Journal of Applied Meteorology* 11, 283–297.
- Draxler, R.R., Rolph, G.D., 2013. HYSPLIT (HYbrid Single-Particle Lagrangian Integrated Trajectory) Model access via NOAA ARL READY Website (<http://ready.arl.noaa.gov/HYSPLIT.php>). NOAA Air Resources Laboratory, Silver Spring, MD.
- Hopmans, E.C., Weijers, J.W.H., Schefuß, E., Herfort, L., Sinninghe Damsté, J.S., Schouten S., 2004. A novel proxy for terrestrial organic matter in sediments based on branched and isoprenoid tetraether lipids. *Earth Planetary Science Letters* 224, 107–116.
- Kim, J.-H., Meer, J.v.d., Schouten, S., Helmke, P., Willmott, V., Sangiorgi, F., Koç, N., Hopmans, E.C., Sinninghe Damsté, J.S., 2010. New indices and calibrations derived from the distribution of crenarchaeol isoprenoid tetraether lipids: implications for past sea surface temperature reconstructions. *Geochimica et Cosmochimica Acta* 74, 4639–4654.
- Peterse, F., van der Meer, J., Schouten, S., Weijers, J.W.H., Fierer, N., Jackson, R.B., Kim, J.-H., Sinninghe Damsté, J.S., 2012. Revised calibration of the MBT–CBT paleotemperature proxy based on branched tetraether membrane lipids in surface soils. *Geochimica et Cosmochimica Acta* 96, 215–229.
- Prahl, F.G., de Lange G.J., Scholten, S., Cowie, G.L., 1997. A case of postdepositional aerobic degradation of terrestrial organic matter in turbidite deposits from the Madeira Abyssal Plain. *Organic Geochemistry* 27, 141 – 152.
- Prahl, F.G., Cowie, G.L., De Lange, G.J., Sparrow, M.A., 2003. Selective organic matter preservation in "burn-down" turbidites on the Madeira Abyssal Plain. *Paleoceanography* 18, doi:10.1029/2002PA000853.
- Schefuß, E., Ratmeyer, V., Stuut, J.-B. W., Jansen, J.H.F., Sinninghe Damsté, J.S., 2003. Carbon isotope analysis of n-alkanes in dust from the lower atmosphere over the central eastern Atlantic. *Geochimica et Cosmochimica Acta* 67, 1757-1767.
- Schouten, S., Hopmans, E.C., Schefuß, E., Sinninghe Damsté, J.S., 2002. Distributional variations in marine crenarchaeotal membrane lipids: a new organic proxy for reconstructing ancient sea water temperatures? *Earth and Planetary Science Letters* 204, 265–274.
- Stuut, J.-B., Zabel, M., Ratmeyer, V., Helmke, P., Schefuß, E., Lavik, G., Schneider, R., 2005. Provenance of present-day eolian dust collected off NW Africa, *Journal of Geophysical Research: Atmospheres* 110, D04202.